

# Iron(II) Spin Transition Complexes with Dendritic Ligands, Part I

Prashant Sonar,<sup>[a]</sup> C. Matthias Grunert,<sup>[b]</sup> Yong-Li Wei,<sup>[b]</sup> Joachim Kusz,<sup>[b,c]</sup>  
Philipp Gülich,<sup>\*[b]</sup> and A. Dieter Schlüter<sup>\*[a]</sup>

*Dedicated to Prof. Dieter Fenske on the occasion of his 65th birthday*

**Keywords:** Fe<sup>II</sup> spin crossover / Dendron complexes / Mössbauer spectroscopy / Magnetic susceptibility / XRD / DSC measurements

The ligands G1- and G2-oligo (benzyl ether) (PBE) dendrons and their iron(II) complexes [Fe(Gn-PBE)<sub>3</sub>]<sub>A</sub><sub>2</sub>·xH<sub>2</sub>O (with n = 1, 2 and A = triflate, tosylate) were prepared. The magnetic properties of the complexes were investigated by a SQUID magnetometer. All complexes exhibit gradual spin transition below room temperature. At very low temperatures the magnetic behaviour reflects zero-field splitting (ZFS) effects. <sup>57</sup>Fe-Mössbauer spectroscopy was performed to distinguish

between ZFS of high spin species and spin state conversion into the low spin state. Further characterisation was carried out by thermogravimetric analysis (TGA) and FT-IR spectroscopy. Structural features have been determined by powder XRD measurements.

(© Wiley-VCH Verlag GmbH & Co. KGaA, 69451 Weinheim, Germany, 2008)

## Introduction

Transition metal complexes with spin crossover (SCO) behaviour have been studied since the last seven decades and the field has been widely reviewed.<sup>[1]</sup> Particularly extensive work has been published about iron(II) SCO complexes with thermal high spin (HS, <sup>5</sup>T<sub>2</sub>) ↔ low spin (LS, <sup>1</sup>A<sub>1</sub>) transition describing the SCO behaviour as influenced by chemical alteration (ligand substitution, nature of anion and crystal solvent, metal dilution) and physical perturbation (light, pressure, magnetic field).<sup>[2]</sup> One of the main objectives has been to learn as much as possible about the mechanism of SCO and the cooperative interactions<sup>[1–4]</sup> that are responsible for the appearance of different types of spin-transition curves  $\gamma_{\text{HS}}(T)$ , the plot of the molar fraction of the high-spin molecules as a function of temperature, which varies from gradual to abrupt and exhibits sometimes hysteresis and incomplete transitions.<sup>[2]</sup> Another recently pursued objective is the attempt to combine SCO with another dynamical physical phenomenon such as nonlinear optical or liquid crystalline properties in one and the same

compound.<sup>[5–7]</sup> SCO compounds exhibiting spin state changes in the room temperature region have attracted particular interest in recent years because of their possible use in sensors and optical devices. Suitability of such material for practical applications<sup>[8]</sup> depends strongly on its chemical stability. This aspect is particularly important in the case of iron(II) complexes because of their tendency to oxidise more or less easily in ambient atmosphere. In recent years researchers have been seeking for new synthetic strategies for the preparation of SCO compounds with special emphasis on steering the cooperative interactions towards room temperature switching operation on the one hand and reaching sufficient chemical stability for long term practical use in ambient atmosphere on the other hand.<sup>[9–11]</sup> Special attention has thereby been paid to the role of dimensionality of the lattice network and the way of interconnecting building blocks by  $\pi$ -interaction and/or hydrogen bonding. Promising approaches include also embedding a spin transition complex into polymer films, e.g. Nafion films<sup>[12]</sup> by which the counterions for the cationic SCO complex are supplied, or attaching the complexes directly to a polymeric chain via ligand interaction as reported by Maeda et al.<sup>[13]</sup>

Our attention has recently been drawn to dendritic systems which could eventually be capable of complex formation with iron(II) ions via nitrogen donor atoms in 4-position of 1,2,4-triazole molecules as “zero-generation basis”. Many SCO compounds of iron(II) based on 1,2,4-triazole ligands have been reported,<sup>[1]</sup> and it has turned out that these are among the most stable ones known so far, which in fact have already been turned into prototypes of de-

[a] Laboratory of Polymer Chemistry, Department of Materials, Swiss Federal Institute of Technology, ETH Zürich, HCI J541, 8093 Zürich, Switzerland  
E-mail: dieter.schluter@mat.ethz.ch

[b] Institut für Anorganische Chemie und Analytische Chemie, Johannes Gutenberg Universität Mainz, Staudingerweg 9, 55099 Mainz, Germany  
Fax: 49-6131-3922990  
E-mail: guetlich@uni-mainz.de

[c] University of Silesia, Institute of Physics, ul. Uniwersytecka 4, 40007 Katowice, Poland

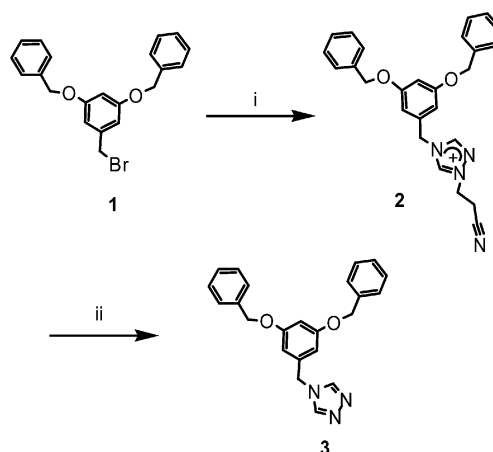
vices.<sup>[8]</sup> Hoping that iron(II) SCO compounds with triazole-based dendritic ligands would combine new spin transition properties suitable for practical use with satisfactory chemical stability we have started the work presented here. Dendritic materials are regularly branched compounds with high molecular weight. They provide a defined number of end groups, whose modification allows to “fine tune” their properties. Among them dendronized polymers are one class of materials in which dendrons are connected to every repeating unit of the linear backbone of a polymeric chain.<sup>[14]</sup> They have been individualized on solid substrates and moved about with the scanning force microscopy tip.<sup>[15]</sup> If one were to use dendronized triazoles as ligand in spin-transition polymers, a material could be obtained which in an ideal way combines the properties of dendronized polymers (high solubility, good processability) with the physical properties of transition metal complexes. A first step in this direction has been accomplished by Fujigaya<sup>[16]</sup> who presented dendronized iron(II) complexes of the kind iron(II)-tris[*Gn*-poly(benzyl ether)dendron] methyl sulfonic acid (*Gn*, *n* = 0, 1, 2). These dendronized coordination polymers turned out to be magnetically active, however, the conversion of low to high spin states was irreversible due to an irreversible loss of water during the first heating process leading to the spin change. Stimulated by this experiment we set out in a long-term project to try to find reversible spin-transition-dendronized polymers which, when individualized on a substrate would change colour depending upon their state of bending. This work reports as a step towards these goals the synthesis of first- (G1) and second-generation (G2) Fréchet/Hawker-type dendronized triazole complexes of the kind [Fe(G1,2-PBE)]A<sub>2</sub>·xH<sub>2</sub>O where G1-PBE denotes 4-[3,5-bis(benzyloxy)benzyl]-4*H*-1,2,4-triazole and G2-PBE represents 4-{3,5-bis[3,5-bis(benzyloxy)benzyl]benzyl}-4*H*-1,2,4-triazole as ligands. Toluenesulfonate (tos) and trifluorosulfonate (trif) were used as counterions (A).

## Results and Discussion

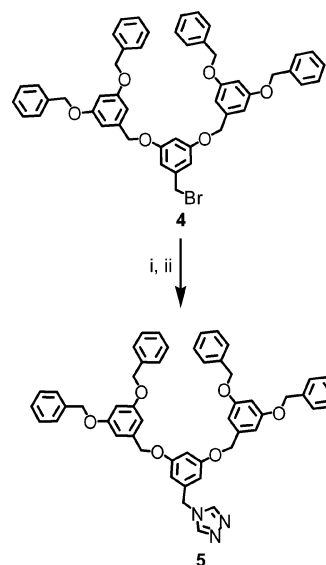
### Synthesis of the Ligands

Alkylation of 1,2,4-triazoles leads to mixtures of 1- and 4-substituted products<sup>[17]</sup> which can be circumvented by the elegant Horváth method.<sup>[18]</sup> Here parent azoles are first protected at N-1 by reacting them with, for instance, acrylonitrile to give the corresponding Michael adducts. Then, they can be selectively alkylated at the desired N-4 to furnish a salt as an intermediate which is subsequently deprotected at N-1 by base-induced elimination. Application of this method to triazole **3** (Scheme 1) started from the Fréchet first-generation (G1) dendron **1** whose benzylic bromide was attached to 1*H*-1,2,4-triazole-1-propanenitrile in refluxing acetonitrile to give intermediate **2** from which the G1 dendritic triazole **3** was obtained by basic treatment in an overall yield of 73%. The purity of **3** was confirmed by <sup>1</sup>H NMR spectroscopy and elemental analysis. The second-generation (G2) triazole **5** was prepared similarly to **3**

using the G2 dendron **4**<sup>[19]</sup> and obtained in a yield of 61% (Scheme 2) after treating the ionic intermediate (not shown) with sodium hydroxide in a dichloromethane/water mixture (4:1).



Scheme 1. Reagents and conditions of (i) 1*H*-1,2,4-triazole-1-propanenitrile, acetonitrile, reflux, 12 h, 80% and (ii) dichloromethane/water (4:1), NaOH, room temp., 5 h; 73%.



Scheme 2. Reagents and conditions of (i) 1*H*-1,2,4-triazole-1-propanenitrile, acetonitrile, reflux, 12 h, 80% and (ii) dichloromethane/water (4:1), NaOH, room temp., 5 h; 61%.

### Synthesis of the Complexes

The complexation of iron(II) triflate or tosylate salt with the ligands **3** or **5** in methanol and precipitation by addition of tetrahydrofuran (THF) yielded the following complexes: [Fe(G1-PBE)<sub>3,7</sub>](trif)<sub>2</sub>·1H<sub>2</sub>O, [Fe(G1-PBE)<sub>3</sub>](tos)<sub>2</sub>·4H<sub>2</sub>O, [Fe(G2-PBE)<sub>3,4</sub>](trif)<sub>2</sub>·4.3H<sub>2</sub>O and [Fe(G2-PBE)<sub>2,7</sub>](tos)<sub>2</sub>·2.9H<sub>2</sub>O. More details concerning the synthesis and the characterisation of the complexes (elemental analysis, neutron activation analysis, thermogravimetric analysis and infrared spectroscopy) are given in the Exp. Section.

### Differential Scanning Calorimetry

The loss of water, as observed by thermo-gravimetric analysis (see Exp. Section) can also be found in measurements with differential scanning calorimetry (DSC) during the first heating process. Figure 1 (a) presents the data obtained for  $[\text{Fe}(\text{G1-PBE})_{3,7}](\text{triflate})_2 \cdot \text{H}_2\text{O}$ . The graph shows for the first heating process of the sample a complex overlapping of endothermic signals between about 40 and 95 °C with peak maxima at 50 °C and 80 °C, which points to a combined process of releasing water, structural rearrangements and eventually a partial spin state change. This will be superimposed by structural changes of the sample which was prepared at low temperature and, therefore, will not have been in its energy minimum structure. Caused by the overlapping and not distinguishable effects only a qualitative analysis will be discussed. Repeated cooling and heating leads to a reversible phase transition at approximately 46 °C in the cooling and 54 °C in the heating mode. Figure 1 (b) depicts DSC data obtained for  $[\text{Fe}(\text{G1-PBE})_3](\text{tos})_2 \cdot 4\text{H}_2\text{O}$ . The temperature behaviour is similar to the previous complex. In the first heating period a phase transition at about 45 °C over a range of 30 °C and the endothermic peak of the evaporating solvent at 100 °C can be found. At

about 240 °C an additional endothermic signal is detected. In the cooling procedure the sample gives an exothermic response at this temperature. Further cooling leads to a phase transition at about 38 °C which is similar to the previous sample. This phase transition is reversible and appears during the following heating process at about 48 °C.

For the complexes of the second generation, G2-PBE, the first heating process is also irreversible as can be seen in Figure 1 (c). The DSC data show a strong endothermic signal between about 30 °C and 100 °C with contribution of several processes and a very pronounced peak at 48 °C in the case of  $[\text{Fe}(\text{G2-PBE})_{3,4}](\text{triflate})_2 \cdot 4.3\text{H}_2\text{O}$  and 49 °C in the case of  $[\text{Fe}(\text{G2-PBE})_{2,7}](\text{tosylate})_2 \cdot 2.9\text{H}_2\text{O}$ . These strong signals below 50 °C might be already the effect of evaporating water. Therefore, it is possible that also complexes of G2 generation exhibit a release of water in two steps. The latter compound shows an additional endothermic peak at 179 °C (Figure 1, d). In this case it seems that the second signal compensates for the first exothermic signal and might also be an effect of structural rearrangements. After the first heating procedure, the picture is similar to the behaviour of the tempered complexes with G1-PBE ligands. The triflate complex has a phase transition at

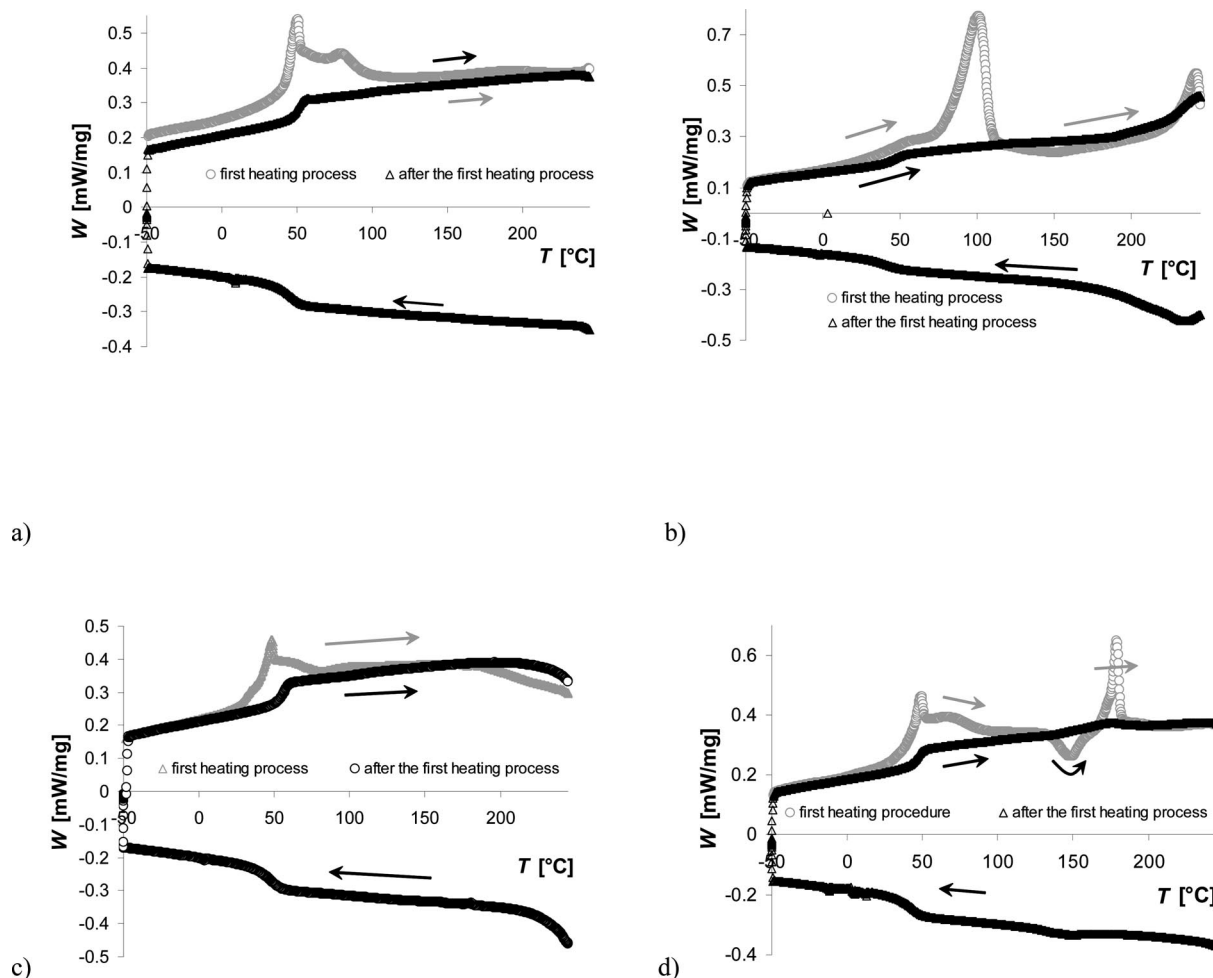


Figure 1. Thermodynamic behaviour of a)  $[\text{Fe}(\text{G1-PBE})_{3,7}](\text{triflate})_2 \cdot \text{H}_2\text{O}$ , b)  $[\text{Fe}(\text{G1-PBE})_3](\text{tos})_2 \cdot 4\text{H}_2\text{O}$ , c)  $[\text{Fe}(\text{G2-PBE})_{3,4}](\text{triflate})_2 \cdot 4.3\text{H}_2\text{O}$ , and d)  $[\text{Fe}(\text{G2-PBE})_{2,7}](\text{tos})_2 \cdot 2.9\text{H}_2\text{O}$ .

about 45 °C and the complex with tosylate counterion shows a hysteresis with 49 °C in the cooling and 54 °C in the heating mode.

### Powder X-ray Diffraction Experiments

The result of the X-ray powder experiment with a fresh sample of  $[\text{Fe}(\text{G1-PBE})_3](\text{tos})_2 \cdot 4\text{H}_2\text{O}$  measured at 300 K shows a pronounced powder diffraction pattern in the measured range of angles  $2\theta$  between 2° and 20° (Figure 2). From this the unit cell can be determined as triclinic with  $a = 20.445 \text{ \AA}$ ,  $b = 16.719 \text{ \AA}$ ,  $c = 12.164 \text{ \AA}$  and  $\alpha = 85.94^\circ$ ,  $\beta = 107.91^\circ$  and  $\gamma = 96.031^\circ$ . The volume of a unit cell containing  $Z = 2$  formula units is  $3931.1 \text{ \AA}^3$  leading to a density of  $\rho = 1.34 \text{ g/cm}^3$ . This differs from the results obtained by Fujigaya<sup>[16]</sup> and Seredyuk<sup>[7]</sup> for similar iron(II) dendritic and liquid crystalline systems who found hexagonal structures. The other possible interpretation of the fresh  $[\text{Fe}(\text{G1-PBE})_3](\text{tos})_2 \cdot 4\text{H}_2\text{O}$  sample phase is to assume two different two-dimensional hexagonal phases, the first with lattice parameter  $a = 19.30 \text{ \AA}$  and the second with  $a = 22.73 \text{ \AA}$ . The experimental results do not allow to distinguish between both cases.

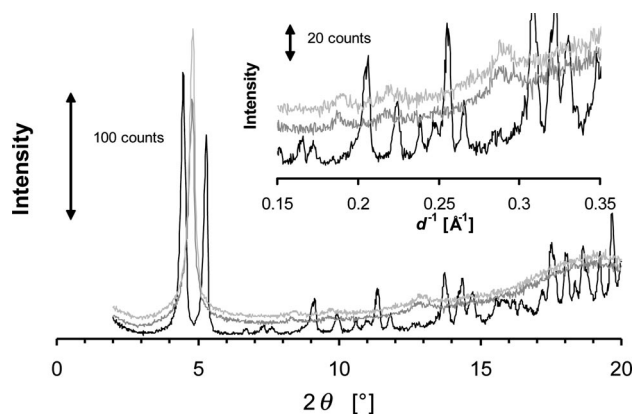


Figure 2. X-ray powder diffraction pattern of a fresh sample of  $[\text{Fe}(\text{G1-PBE})_3](\text{tos})_2 \cdot 4\text{H}_2\text{O}$  measured at 300 K (dark grey), at 350 K (grey) and at 300 K after heat treatment (light grey).

However, when the sample is heated to 350 K the structure changes due to the loss of water (Figure 2). One strong reflection appears at  $2\theta = 4.807^\circ$ , a broad halo is visible at about 20°, originating from the voluminous dendritic branches, and some small reflections are at  $8.334^\circ$ ,  $9.626^\circ$  and  $12.746^\circ$ . After cooling to 300 K the positions of these reflections changed slightly. The first reflection appears at  $2\theta = 4.821^\circ$  and some small reflections are at  $8.356^\circ$ ,  $9.651^\circ$  and  $12.779^\circ$ . The reflections can be indexed as (1, 0), (1, 1), (2, 0) and (2, 1) belonging to a two-dimensional hexagonal lattice with lattice parameters equal to  $18.37 \text{ \AA}$  and  $18.31 \text{ \AA}$  for 350 and 300 K, respectively. Now the structure of the tempered complexes is consistent with the complexes examined by Fujigaya<sup>[16]</sup> and Seredyuk.<sup>[7]</sup> The phase transition upon heating is not reversible and the structure remains stable, when the sample is cooled again to 300 K. These experiments are presented in Figure 2.

Figure 3 shows the experiments performed with a fresh sample of the G2 compound,  $[\text{Fe}(\text{G2-PBE})_{2.7}](\text{tos})_2 \cdot 2.9\text{H}_2\text{O}$ . The pattern between 2° and 20° shows at 300 K only one broad reflection at  $2\theta = 3.813^\circ$  and a broad halo at about 20° originating from the voluminous dendritic branches. During the heating process to 350 K the complex starts to crystallize and shows a strong reflection at  $2\theta = 3.724^\circ$  and some small reflections at  $6.453^\circ$ ,  $7.452^\circ$  and  $9.864^\circ$ . This crystallization process is irreversible and remains as such after cooling to 300 K, but the reflections changed their position. The first strong reflection is at position  $2\theta = 3.734^\circ$  and some small reflections appear at positions  $6.470^\circ$ ,  $7.473^\circ$  and  $9.891^\circ$ . These reflections could be indexed as (1, 0), (1, 1), (2, 0) and (2, 1) belonging to a two-dimensional hexagonal lattice with lattice parameters  $a = 3.71$  and  $23.64 \text{ \AA}$  for 350 and 300 K, respectively. Comparable results were obtained by Fujigaya<sup>[16]</sup> and Seredyuk.<sup>[7]</sup>

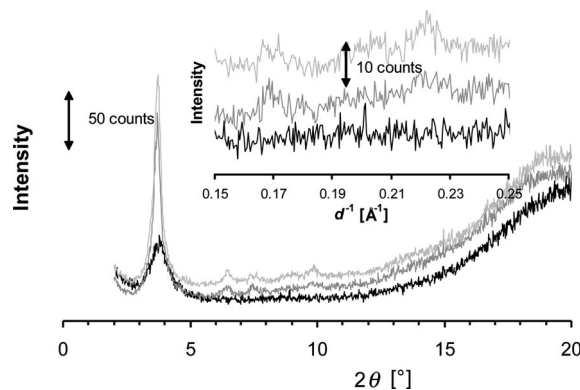


Figure 3. X-ray powder diffraction pattern of a fresh sample of  $[\text{Fe}(\text{G2-PBE})_{2.7}](\text{tos})_2 \cdot 2.9\text{H}_2\text{O}$  measured at 300 K (dark grey), at 350 K (grey) and at 300 K after heat treatment (light grey).

### Magnetic Measurements

The spin transition behaviour as a function of temperature has also been followed by magnetic susceptibility measurements using a SQUID magnetometer with the following temperature program: 4 or 200 or 250 K (for different runs)  $\rightarrow 350 \rightarrow 4 \rightarrow 350 \text{ K}$ .

In the case of  $[\text{Fe}(\text{G1-PBE})_3](\text{trif})_2 \cdot \text{H}_2\text{O}$  in (Figure 4, a) the value of  $\chi_{\text{M}}T$  increases slightly from 2.9 to  $3.1 \text{ cm}^3 \text{ K mol}^{-1}$  upon heating from 200 to 300 K. Between 300 and 350 K, where the sample loses water, the  $\chi_{\text{M}}T$  value increases to ca.  $3.6 \text{ cm}^3 \text{ K mol}^{-1}$ . Values between  $3.0$  and  $3.5 \text{ cm}^3 \text{ K mol}^{-1}$  are typical of iron(II) complexes in the HS state. The calculation of the  $\chi_{\text{M}}T$  values is based on the molecular mass, which was calculated using the iron content determined by neutron activation analysis (see Exp. Section). With respect to the experimental error, the  $\chi_{\text{M}}T$  value of  $3.6 \text{ cm}^3 \text{ K mol}^{-1}$  falls into the expected range for iron(II) HS species. On cooling the sample the  $\chi_{\text{M}}T$  value remains constant until 200 K, which shows that the change of  $\chi_{\text{M}}T$  observed during the first heating process is not fully reversible (Figure 4, a). This is most likely due to loss of water as discussed above. Between 200 and 50 K the sample

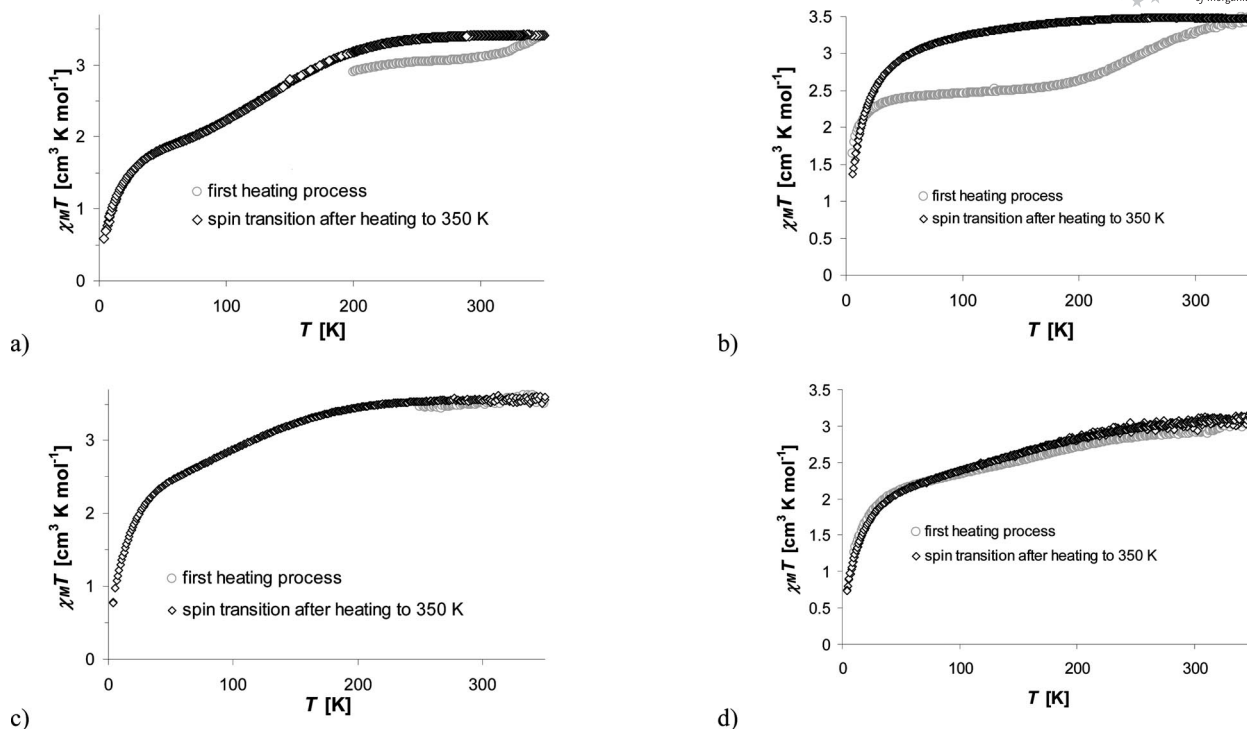


Figure 4. Temperature-dependency behaviour followed by magnetic measurements for a)  $[\text{Fe}(\text{G1-PBE})_{3,7}](\text{triflate})_2 \cdot 1\text{H}_2\text{O}$ , b)  $[\text{Fe}(\text{G1-PBE})_3](\text{tos})_2 \cdot 4\text{H}_2\text{O}$ , c)  $[\text{Fe}(\text{G2-PBE})_{3,4}](\text{triflate})_2 \cdot 4.3\text{H}_2\text{O}$ , and d)  $[\text{Fe}(\text{G2-PBE})_{2,7}](\text{tos})_2 \cdot 2.9\text{H}_2\text{O}$ .

undergoes a gradual spin transition and reaches a  $\chi_{\text{M}}T$  value of  $1.8 \text{ cm}^3 \text{ K mol}^{-1}$ . The rather abrupt decrease of  $\chi_{\text{M}}T$  below 50 K is induced by zero-field splitting. The second heating procedure of the compound results in the same data as measured in the cooling procedure of the respective sample. The gradual spin transition below 200 K is reversible.

During the first heating procedure of  $[\text{Fe}(\text{G1-PBE})_3](\text{tos})_2 \cdot 4\text{H}_2\text{O}$  (see Figure 4, b) the abrupt increase of the  $\chi_{\text{M}}T$  value between 4 and 50 K originates from zero-field splitting. The value of  $\chi_{\text{M}}T$  between 50 and 200 K remains constant at ca.  $2.5 \text{ cm}^3 \text{ K mol}^{-1}$  and increases by further heating to 350 K to  $3.5 \text{ cm}^3 \text{ K mol}^{-1}$ , confirming that the compounds under study are entirely in the HS state. Similar to the previous sample, the spin change is not reversible and the sample remains at ca.  $3.5 \text{ cm}^3 \text{ K mol}^{-1}$  while cooling to 200 K. Below this temperature, the sample undergoes a partial and very gradual spin transition by ca.  $0.3 \text{ cm}^3 \text{ K mol}^{-1}$ . Below 50 K the magnetic curve is dominated again by the effect of zero-field splitting. Similar to the observation on the triflate complex (Figure 4, a), the magnetic behaviour in the second heating procedure follows the behaviour observed in the cooling process.

Complexes with dendritic ligands of the second generation (see parts c and d in Figure 4) do not show pronounced irreversible effects in their magnetic behaviour. The magnetic curve below 50 K is dominated by zero-field splitting, between 50 and 200 K a gradual and only partial spin transition can be observed followed by a plateau above this temperature. The  $\chi_{\text{M}}T$  values at room temperature for

$[\text{Fe}(\text{G2-PBE})_{3,4}](\text{triflate})_2 \cdot 4.3\text{H}_2\text{O}$ , and  $[\text{Fe}(\text{G2-PBE})_{2,7}](\text{tos})_2 \cdot 2.9\text{H}_2\text{O}$  are ca. 3.0 and ca.  $3.5 \text{ cm}^3 \cdot \text{K mol}^{-1}$ , respectively.

The change of spin state during the first heating procedure of the complexes with G1-ligands as displayed in Figure 4 (a, b) resembles the abrupt spin state change during the release of water observed by Fujigaya<sup>[16]</sup> et al. for their dendritic triazole complexes with different ligands, but the effect in their studies is far more pronounced than in ours. The reason may be that Fujigaya et al. used amide groups to bridge the coordinating triazole with the dendritic ligands. These amide groups are able to bind water molecules via hydrogen bonding in the close neighbourhood of the spin state changing iron centre. This very likely affects the spin transition behaviour. In the present study the ligands do not contain such hydrophilic amide groups. Therefore, it is assumed that the water molecules are not localized in the same fashion, but rather distributed over the lattice in positions with less influence on the spin transition behaviour. By the same token, it seems that in the present study the structural rearrangements due to loss of water have less influence on the spin transition behaviour than in Fujigaya's study.

### <sup>57</sup>Fe Mössbauer Spectroscopy

Mössbauer spectroscopy was performed for the tosylate complexes at 80 and 4.2 K using fresh samples before heating above 300 K (Figure 5). Mössbauer effect measurements at room temperature were not possible because of

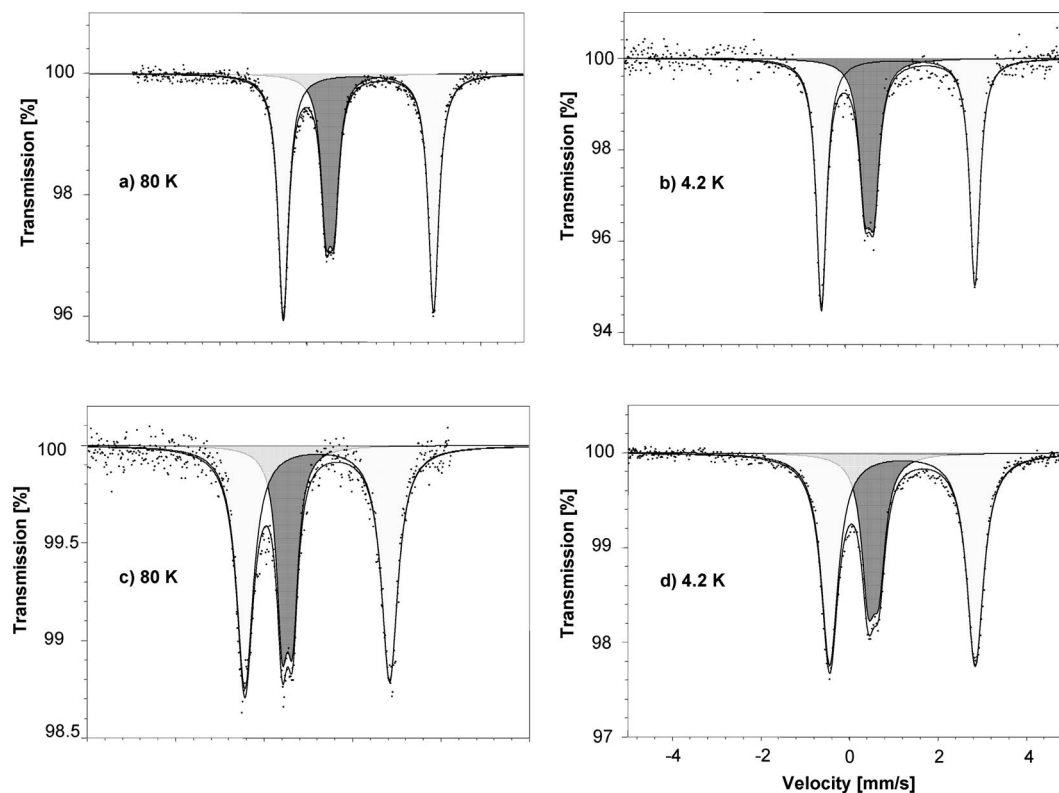


Figure 5. <sup>57</sup>Fe-Mössbauer spectra of [Fe(G1-PBE)<sub>3</sub>](tos)<sub>2</sub>·4H<sub>2</sub>O (a and b) as well as [Fe(G2-PBE)<sub>3</sub>](tos)<sub>2</sub>·2.9H<sub>2</sub>O (c and d).

the softness of the material. Responsible for this softness are the flexible branches in combination with solvent molecules. The high flexibility leads to an abrupt decrease of the Lamb-Mössbauer factor and prevents the acquisition of data of sufficient quality in the room temperature range.

The spectrum of [Fe(G1-PBE)<sub>3</sub>](tos)<sub>2</sub>·4H<sub>2</sub>O recorded at 80 K (Figure 5, a) can be separated into two doublets of Lorentzian lines. One doublet with an isomer shift  $\delta = 1.19$  mm/s and a quadrupole splitting  $\Delta = 3.45$  mm/s refers to iron(II) in the HS state. The large value of the quadrupole splitting is mainly caused by noncubic valence-electron distribution to the electric field gradient and indicates that the lattice contribution to the electric field gradient is relatively small, i.e. the inner core FeN<sub>6</sub> apparently is not significantly distorted. Obviously, the flexible and voluminous dendritic ligands serve as a soft medium embedding the actual chromophores in a relatively unperturbed fashion. A second doublet with  $\delta = 0.54$  mm/s and  $\Delta = 0.19$  mm/s can be attributed to the diamagnetic Fe<sup>II</sup> LS species. The area fraction of the HS doublet being approximately equal to the molar fraction of the HS molecules is  $\gamma_{\text{HS}} = 0.67$ , which

is slightly lower than expected from the magnetic measurements after heating to 350 K. The small deviation (ca. 4%) is possibly due to the slightly higher Debye-Waller factor for the LS species compared to the HS species.<sup>[20,21]</sup> The <sup>57</sup>Fe-Mössbauer spectrum obtained at 4.2 K exhibits similar parameter values as determined at 80 K. The value of  $\gamma_{\text{HS}} = 0.63$  is only slightly lower than at 80 K, which is in agreement with the observed gradual spin transition and proves that the strong decrease of  $\chi_{\text{M}}T$  below 50 K is the result of zero-field splitting. All Mössbauer parameter values are summarized in Table 1. The Mössbauer parameter values measured for the second-generation complex [Fe(G2-PBE)<sub>3</sub>](tos)<sub>2</sub>·2.9H<sub>2</sub>O are very similar. The quadrupole splitting of the HS doublet is somewhat smaller ( $\Delta = 3.27$  mm/s at 80 K) than observed for the G<sub>1</sub> complex. The half width,  $\Gamma$ , of the Lorentzian lines of the HS species of [Fe(G2-PBE)<sub>3</sub>](tos)<sub>2</sub>·2.9H<sub>2</sub>O is 0.46 mm/s and thus significantly higher than the LS signal (about 0.3 mm/s) and observed for the G<sub>1</sub> complex. The smaller quadrupole splitting as compared to that of the G<sub>1</sub> system indicates that the lattice contribution to the electric field gradient is somewhat larger in

Table 1. Parameter of the measured <sup>57</sup>Fe-Mössbauer spectra.

Complexes	Low-Spin State				High-Spin State				% HS area
	<i>T</i> [K]	$\delta$ [mm/s]	$\Delta E_Q^{LS}$ [mm/s]	$\Gamma$ [mm/s]	$\delta$ [mm/s]	$\Delta E_Q^{HS}$ [mm/s]	$\Gamma$ [mm/s]		
[Fe(G1-PBE) <sub>3</sub> ](tos) <sub>2</sub> ·4H <sub>2</sub> O	80	0.54(1)	0.19(1)	0.28(2)	1.19(1)	3.45(1)	0.30(1)	67 (1)	
	4.2	0.55(2)	0.21(2)	0.30(4)	1.20(1)	3.47(1)	0.28(2)	63 (3)	
[Fe(G2-PBE) <sub>3</sub> ](tos) <sub>2</sub> ·2.9H <sub>2</sub> O	80	0.53(1)	0.24(2)	0.30(3)	1.20(1)	3.27(3)	0.46(2)	68 (3)	
	4.2	0.55(1)	0.24(1)	0.36(2)	1.20(1)	3.29(1)	0.46(1)	70 (2)	

the G2 system as a result of the more voluminous ligands giving rise to more steric hindrance. The steric influence on each chromophore is not sharply defined, but rather spread over a certain distribution of distortions. This may be the reason for the larger line width of the HS doublet in the G2 system.

## Conclusions

Fe<sup>II</sup> triazole complexes form mostly 1D-chains using dendritic triazoles as ligands, these chains are well encompassed by dendritic branches. The material properties of these complexes are thus similar to those of the ligands themselves. This is the reason why the preparation of the pure complex compound with Fe<sup>II</sup>/ligand ratio of 1:3 was not possible with the present ligand material. Attempts to fully evaporate a complexation mixture, as done by Fujigaya,<sup>[16]</sup> did not afford well coordinated material. It turned out that the best procedure for the synthesis of PBE dendritic complexes was to precipitate and wash them at low temperature (approx. -80 °C). This, however, made it impossible to guarantee that no additional ligand precipitates together with the complex compound. The iron concentration could be determined by neutron activation analysis, and together with TGA and elemental analysis the correct formula weight was calculated.

Fresh samples of the dendritic iron(II) compounds under study lose crystal water upon heating between 40 and 100 °C with a slight increase of the  $\chi_M T$  value. This is accompanied by structural changes as proven by XRD measurements. The change of  $\chi_M T$  is less pronounced in the present study than in the report of Fujigaya,<sup>[16]</sup> probably due to the fact that in his case the bridging NH group between the triazole and the dendritic branch offers the possibility of binding water molecules with significant influence on the spin state of the iron centre. In our study the systems contain bridging aliphatic groups which do not interact with crystal water molecules, and the expected influence on the spin state of the central iron ion is of minor importance. All dendritic iron(II) compounds under study exhibit a partial and gradual spin transition below 200 K. The spin transition is not complete and the abrupt decrease of  $\chi_M T$  below 50 K originates from zero-field-splitting, which was proven by <sup>57</sup>Fe-Mössbauer spectroscopy.

## Experimental Section

**Materials:** All solvents used for the synthesis of the ligands were dried before use. All reactions were carried out under nitrogen atmosphere with degassed dry solvents and the dendritic triazoles were purified by column chromatography using 300–400 and 100–200 mesh (Macherey–Nagel) silica gel, respectively. 1*H*-1,2,4-triazole-1-propanenitrile was synthesized from 1*H*-1,2,4-triazole and acrylonitrile as described in the literature.<sup>[18]</sup> All the materials necessary for the syntheses of the complexes are commercially available and were used as supplied.

**Methods:** <sup>1</sup>H (300 MHz) and <sup>13</sup>C (62.5 MHz) NMR spectroscopy was carried out on a Bruker type spectrometer at room tempera-

ture. Elemental analysis (C,H,N and S Analyzer) and mass spectroscopy (Ionspec Ultrima spectrometer) techniques were utilized for the confirmation and purity of the ligands. The purity of the complexes was proven by elemental analysis (C, H, N, and S) using a Vario EL of Elementar. The iron content was determined by neutron activation analysis. Samples of the dendronised complexes and iron(II) sulfate as reference were irradiated for 6 h with thermal neutrons in the nuclear research reactor TRIGA Mark (II) (Mainz) at a flux of  $7 \times 10^{11} \text{ n cm}^{-2} \text{ s}^{-1}$  affording the nuclear reaction <sup>58</sup>Fe(n,γ)<sup>59</sup>Fe. After a delay of about two weeks for allowing short-lived radioactive nuclides to decay, the content of <sup>59</sup>Fe with half-life of 44.5 d could be determined by measuring the count rate of γ-radiation (1099 keV and 1293 keV), which is caused by the β-decay to <sup>59</sup>Co. The iron content was given by the ratio of the count rates of the sample and the reference. More details are given in a laboratory report by Grunert et al.<sup>[22]</sup> The complexation of the ligands *Gn*-PBE with their iron(II) salts could also be proven with FT-IR spectroscopy. The experiments were carried out with a Bruker Tensor 27 using samples prepared as KBr pellets. Thermogravimetric analyses were performed by using a Q500 thermogravimetry analyzer (TA Instruments, New Castle, Delaware). The measurements were carried out in nitrogen atmosphere with a heating rate of 10 K/min and confirm the existence of included solvent. Thermodynamic data were obtained by differential scanning calorimetry (DSC) on DSC7 instrument (Perkin–Elmer, Norwalk, Connecticut) with heating and cooling rates of 10 K/min. For structural investigations powder X-ray diffractograms were recorded at 300 K, 350 K and then again at 300 K with Cu-*K<sub>α</sub>* radiation using PANalytical X'Pert PRO diffractometer equipped with the Paar HTK 1200. For the determination of the spin state magnetic measurements were performed using a MPMSXL Quantum Design SQUID magnetometer between 5 K and 350 K at heating and cooling rates of 2 K/min. The measured data were corrected for the magnetisation of the sample holder as well as for their own diamagnetic contribution. Furthermore, <sup>57</sup>Fe Mössbauer spectroscopy was carried out at 80 K using a constant-acceleration conventional spectrometer with a nitrogen cryostat. The source used was <sup>57</sup>Co in a Rh-matrix with an activity of about 10 mCi kept at room temperature. For measurements at 4.2 K the samples were immersed in helium gas in a helium cryostat. In this case the used source was <sup>57</sup>Co in a Rh-matrix with an activity of about 5 mCi kept at 4 K. It was impossible to record Mössbauer spectra at room temperature because of the softness of the material causing too low resonance effects in meaningful measuring times. The isomer shift values are given with reference to α-iron.

### Synthesis of the Ligands

**Compound 3 (G1-PBE):** A one-neck flask was charged with 5.0 g of 1 (13.04 mmol), 1.61 g of 1*H*-1,2,4-triazole-1-propanenitrile (3.13 mmol), and 150 mL of acetonitrile. The mixture was stirred and heated to 88 °C for 20 h under nitrogen. After cooling to room temperature, the solvent was removed by evaporation. The residue was dispersed in 20 mL of diethyl ether; after vigorous stirring for 1 h the ether was decanted. The washing procedure was repeated three times. The residue was dissolved in 20 mL of aq. NaOH (2 M) and stirred overnight at room temperature for deprotection, and after dilution with 200 mL of water, it was extracted with chloroform (300 mL). The organic phase was dried with MgSO<sub>4</sub> and the solvent was removed by evaporation. The crude product was purified by column chromatography using a CHCl<sub>3</sub>/CH<sub>3</sub>OH mixture (95:05). The compound was dried under high vacuum to give 3.00 g of white G1-PBE (3) (yield 73%). <sup>1</sup>H NMR (CDCl<sub>3</sub>): δ = 8.18 (s, 2 H, TrZ), 7.41–7.35 (m, 10 H, Ph), 6.63 (s, 1 H, Ph), 6.40 (s, 2 H, Ph), 5.09–5.02 (m, 6 H, 2Ph-CH<sub>2</sub>, 1 NCH<sub>2</sub>) ppm. <sup>13</sup>C NMR

(CDCl<sub>3</sub>):  $\delta$  = 160.65, 139.46, 136.31, 128.64, 128.58, 128.16, 127.44, 127.09, 106.88, 102.28, 70.27, 70.16, 49.03 ppm. MALDI-TOF mass calcd. for C<sub>23</sub>H<sub>21</sub>N<sub>3</sub>O<sub>2</sub>: [M + H] + 371.44; found 371. C<sub>23</sub>H<sub>21</sub>N<sub>3</sub>O<sub>2</sub> (371.44): calcd. C 74.37, H 5.70, N 11.31; found C 74.20, H 5.23, N 11.17.

**Compound 5 (G2-PBE):** A one-neck flask was charged with 2.0 g 4 (2.47 mmol), 1*H*-1,2,4-triazole-1-propanenitrile 0.307 g (2.47 mmol) and 80 mL of acetonitrile. The mixture was stirred and heated to 88 °C for 20 h. After cooling to room temperature, the solvent was removed by evaporation. The residue was dispersed in 30 mL of diethyl ether; after vigorous stirring for 1 h the ether was decanted. The washing procedure was repeated three times. The residue was dissolved in 15 mL of aq. NaOH (2 M) and stirred for overnight at room temperature for deprotection, and after dilution with 200 mL of water, it was extracted with chloroform (300 mL). The organic phase was dried with MgSO<sub>4</sub> and the solvent removed by evaporation. The crude product was purified by column chromatography using CHCl<sub>3</sub>/CH<sub>3</sub>OH mixture in the ratio of 95:05. The compound was dried under high vacuum and gave 1.2 g of G2-PBE 5 (yield 61%). <sup>1</sup>H NMR (CDCl<sub>3</sub>):  $\delta$  = 8.12 (s, 2 H, Trz), 7.38–7.30 (m, 20 H, Ph), 6.61–6.50 (m, 6 H, Ph), 6.32 (s, 3 H, Ph), 5.01 (s, 12 H, 6CH<sub>2</sub>Ph), 4.90 (s, 2 H, NCH<sub>2</sub>) ppm. <sup>13</sup>C NMR (CDCl<sub>3</sub>):  $\delta$  = 160.12, 139.01, 138.78, 136.81, 128.53, 127.95, 127.53, 108.18, 106.56, 101.75, 70.13, 29.66 ppm. MALDI-TOF mass calcd. for C<sub>51</sub>H<sub>45</sub>N<sub>3</sub>O<sub>6</sub>: [M + H] + 795.94; found 796. C<sub>51</sub>H<sub>45</sub>N<sub>3</sub>O<sub>6</sub>: calcd. C 76.96, H 5.70, N 5.28; found C 76.35, H 5.43, N 5.34.

**Synthesis of the Complexes:** For the preparation of the complexes a methanol solution of the iron(II) triflate and tosylate, respectively, containing a small amount of ascorbic acid to avoid oxidation of iron(II) to iron(III) was added dropwise into a THF solution of the ligand with a molar ratio of iron to ligand of 1:3 at 60 °C. The reaction mixture was stirred at this temperature for about 30 min, then cooled down to room temperature. Part of the solvent was removed under reduced pressure until the solution was separated into two layers. The solution with the pink gelatine like product was cooled with liquid nitrogen to about –50 °C to –100 °C. In that temperature region the product became solid and inflexible and could be collected and washed with cold methanol. The complexes were dried at room temperature.

Elemental analysis (C, H, N and S) was carried out by conventional combustion analysis; the iron content was determined by neutron activation analysis. The amount of iron was used to determine the molecular weight per formula unit of one complex (which corresponds to the repeat unit of Fe triazole chains). TG analysis was used to quantify the solvent content (see the following section). The remaining molecular weight was assigned to the respective ligand and the following values were obtained. They match the calculated ones. Deviations in the ratio of iron to ligand from the theoretical ratio of 1:3 of infinite 1D iron triazole complex chains are due to the conditions during the synthesis and will be discussed above.

**[Fe(G1-PBE)<sub>3.7</sub>](trif)<sub>2</sub>·1H<sub>2</sub>O:** Yield 40.9%. C<sub>87</sub>H<sub>80</sub>F<sub>6</sub>FeN<sub>11</sub>O<sub>14</sub>S<sub>2</sub> (1764): calcd. C 59.91, H 4.60, N 8.90, S 3.67, Fe 3.20; found C 59.69, H 5.02, N 8.81, S 3.74, Fe 3.16.

**[Fe(G1-PBE)<sub>3</sub>](tos)<sub>2</sub>·4H<sub>2</sub>O:** Yield 92.6%. C<sub>83</sub>H<sub>85</sub>FeN<sub>9</sub>O<sub>16</sub>S<sub>2</sub> (1585): calcd. C 62.91, H 5.41, N 7.96, S 4.05, Fe 3.52; found C 63.90, H 5.40, N 7.92, S 3.91, Fe 3.39.

**[Fe(G2-PBE)<sub>3.4</sub>](trif)<sub>2</sub>·4.3H<sub>2</sub>O:** Yield 56.2%. C<sub>175</sub>H<sub>162</sub>F<sub>6</sub>FeN<sub>10</sub>O<sub>31</sub>S<sub>2</sub> (3137.61): calcd. C 67.14, H 5.19, N 4.55, S 2.044, Fe 1.78; found C 66.67, H 5.28, N 4.55, S 1.87, Fe 1.79.

**[Fe(G2-PBE)<sub>2.7</sub>](tos)<sub>2</sub>·2.9H<sub>2</sub>O:** Yield 63.5%. C<sub>152</sub>H<sub>141</sub>FeN<sub>8</sub>O<sub>25</sub>S<sub>2</sub> (2600): calcd. C 70.09, H 5.48, N 4.36, S 2.47, Fe 2.15; found C 70.00, H 6.27, N 4.15, S 1.77, Fe 2.15.

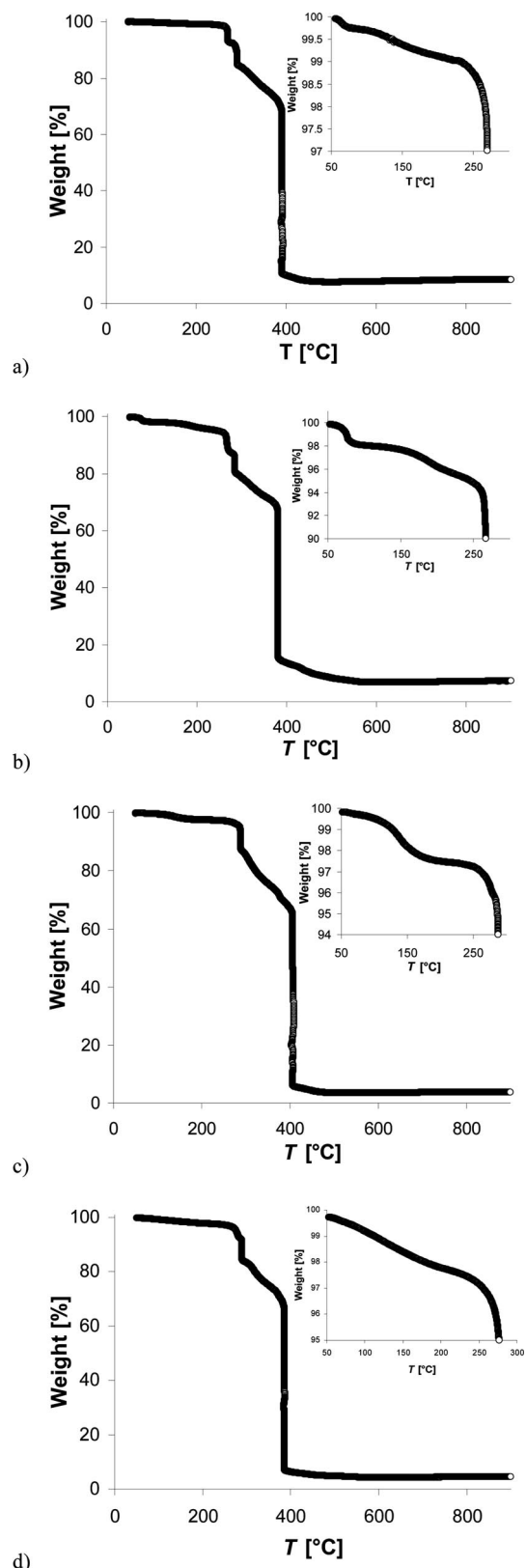


Figure 6. Thermogravimetric analysis of a) [Fe(G1-PBE)<sub>3.7</sub>](trif)<sub>2</sub>·1H<sub>2</sub>O, b) [Fe(G1-PBE)<sub>3</sub>](tos)<sub>2</sub>·4H<sub>2</sub>O, c) [Fe(G2-PBE)<sub>3.4</sub>](trif)<sub>2</sub>·4.3H<sub>2</sub>O and d) [Fe(G2-PBE)<sub>2.7</sub>](tos)<sub>2</sub>·2.9H<sub>2</sub>O.

### Characterization of the Complexes

**Thermogravimetric Analysis (TGA):** TGA confirmed the existence of included solvent, which comes from the synthesis and similar systems are reported in the literature,<sup>[16,7]</sup> in our system we also confirm the solvent as most likely water. The heating curves showed two steps, one at approximately 80 °C and the other at 150 °C (Figure 6, a–d, expanded insets).

This may indicate two different positions in the lattice. The loss of 1% of mass in  $[\text{Fe}(\text{G1-PBE})_3](\text{triflate})_2 \cdot x\text{H}_2\text{O}$  corresponds to about one water molecule (Figure 6, a). The analogous tosylate compound (Figure 6, b) exhibits a mass loss of 4.5% corresponding to approximately four water molecules per formula unit. Complexes with G2 ligands did not show the first pronounced step of mass

reduction at about 80 °C, but at 150 °C a weight loss of 2.5% corresponding to ca. 3.8 molecules of water in the case of  $[\text{Fe}(\text{G2-PBE})_3](\text{triflate})_2 \cdot x\text{H}_2\text{O}$ .  $[\text{Fe}(\text{G2-PBE})_3](\text{tosylate})_2 \cdot x\text{H}_2\text{O}$  shows a gradual release of 2% of its mass which fits to 2.9 water molecules. All four complexes are stable up to about 260 °C, with small deviations of a few degrees between the species. Above this temperature the complexes decompose in small steps. The main decomposition takes place very rapidly around 380 °C and 410 °C.

**FT-Infrared Spectroscopy (IR):** Figure 7 shows the IR spectra of the ligands G1-PBE and G2-PBE as well as their complexes with triflate and tosylate anions. This overview proves the complexation of the iron salts with the ligands and gives first hints for a partial band assignment by comparing the spectra of the free ligands and

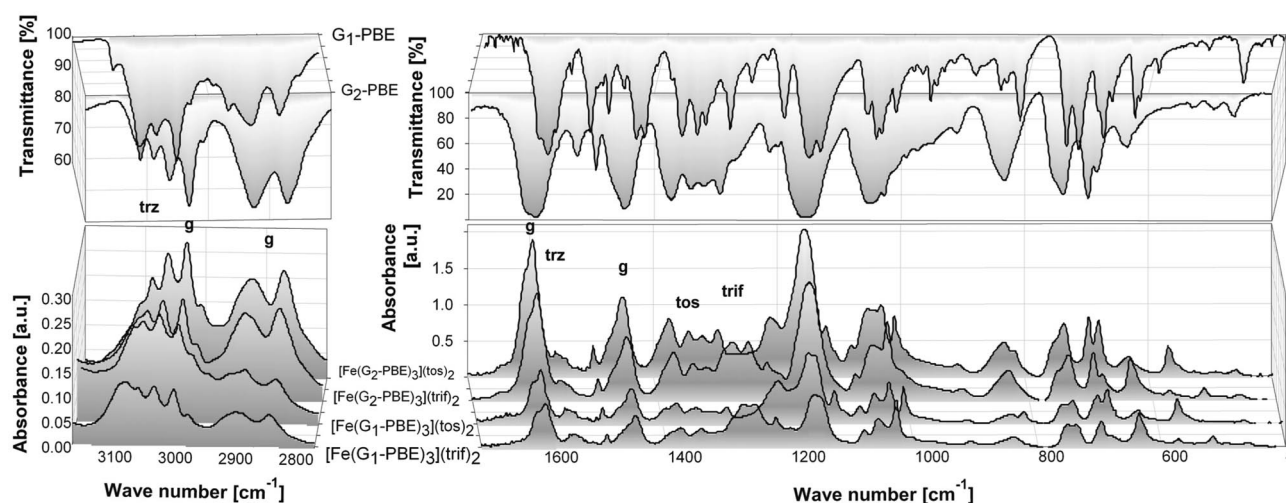


Figure 7. IR spectra of ligands and complexes exhibit differences due to the respective generation (g) and various counterions (trif or tos) for the complexes. Triazole bands (trz) are almost not affected in the different compounds, but often covered by other bands. Band overlaps e.g. in the case of the counterions make assignment more difficult.

Table 2. Band assignment of selected absorption bands for the free dendritic ligands and their iron(II) complexes.

	G1-PBE	G2-PBE	$[\text{Fe}(\text{G1-PBE})_3](\text{trif})_2 \cdot \text{H}_2\text{O}$	$[\text{Fe}(\text{G1-PBE})_3](\text{tos})_2 \cdot 4\text{H}_2\text{O}$	$[\text{Fe}(\text{G2-PBE})_3](\text{trif})_2 \cdot 4.3\text{H}_2\text{O}$	$[\text{Fe}(\text{G2-PBE})_3](\text{tos})_2 \cdot 2.9\text{H}_2\text{O}$
$\nu_{\text{trz}}(\text{C-H})$	3134 vw 3090 w	3112 vw 3088 vw	1314 vw 3092 w	1308 vw 3090 w	1310 vw 3090 w	1310 vw 3088 w
$\nu_{\text{ar}}(\text{C-H})$	3064 w 3031 w 3010 vw	3063 w 3031w 3008 vw	3065 w 3033 w 3009 vw	3064 w 3032 w 3010 vw	3065 w 3032 w 3010 vw	3063 w 3032 w 3008 vw
$\nu_{\text{alk}}(\text{C-H})$	2946 w 2910 w 2864 w	2925 w 2871 w	2930 w 2875 w	2922 w 2871 w	2929 w 2872 w	2923 w 2871 w
$\nu_{\text{ar}}(\text{C=C})$	1612 m 1598 vs 1585 m	1608 m 1595vs	1609 m 1596vs	1609 m 1596 vs	1608 m 1597vs	1608 m 1597vs
$\nu(\text{N=C-N})$	1559 vw	1560 vw	1558 vw	1559 vw	1557 vw	1559 vw
$\delta(\text{CH}_2)$	1454 m 1441 m	1452 s	1452 s	1452 s	1451 s	1452 s
$\nu(\text{C-F})$	–	–	1259 m	–	1255 m	–
$\nu_{\text{asym}}(\text{O=S=O})$	–	–	1277 m	1212 m	1281 m	1214 m
$\nu_{\text{sym}}(\text{O=S=O})^{[a]}$	–	–	<sup>[a]</sup>	1123 w	<sup>[a]</sup>	1123 w
$\nu(\text{C}_{\text{ar}}-\text{O})^{[b]}$	1174 vs	1157vs <sup>[b]</sup>	1163 s	1165 s	1156vs <sup>[b]</sup>	1157vs <sup>[b]</sup>
$\nu(\text{C}_{\text{alk}}-\text{O})^{[b]}$	1155 s	–	1154 s	1155 s	–	–
$\delta_{\text{asym}}(\text{O=S=O})$	–	–	–	681 m	–	680 m
$\gamma(\text{trz})^{[c]}$	634 w	632 w	638 m <sup>[c]</sup>	632 w	636 m	632 w <sup>[c]</sup>
$\delta_{\text{sym}}(\text{O=S=O})$	–	–	<sup>[c]</sup>	568 m	<sup>[c]</sup>	568 m

[a]  $\nu_{\text{sym}}$  overlaps with  $\nu(\text{C-O})$  in case of A = triflate. [b]  $\nu(\text{C}_{\text{ar}}-\text{O})$  and  $\nu(\text{C}_{\text{alk}}-\text{O})$  overlap in case of G2-PBE. [c]  $\gamma(\text{trz})$  overlaps with  $\delta_{\text{sym}}(\text{O=S=O})$  in case of A<sup>-</sup> = triflate.

the ligands in the coordination sphere around the iron centre. Further information for the band assignment was based on literature by Socrates<sup>[23]</sup> and Fujigaya.<sup>[16]</sup>

The bands in the νC–H stretching region of around 3000 cm<sup>-1</sup> were assigned by intensity considerations. Whereas the C–H stretching intensity of the triazole unit should stay constant that of the dendron should increase with the generation. Therefore, the bands between 2800 and 3050 cm<sup>-1</sup> were assigned to the dendron and those at about 3100 cm<sup>-1</sup> to triazole.

A similar picture can be found in the region between 400 and 1700 cm<sup>-1</sup>. Bands of the triazole ring do not exhibit significant differences between first and second generation (e.g. 1498, 695 cm<sup>-1</sup>), while the bands of the benzyl ether show a stronger absorption for the G2-PBE (e.g. around 1600, 1380, and 830 cm<sup>-1</sup>). Beside these differences, the spectra of the complexes also include bands of their respective counterions. They occur for instance at 1260, 637 and 518 cm<sup>-1</sup> in the case of triflate and at 1213, 1011 and 568 cm<sup>-1</sup> for tosylate. More details can be found in Table 2. A complete band assignment was not attempted because of overlap and general complexity. Furthermore, all complexes contain a small amount of water in the lattice giving rise to the typical broad band around 3400 cm<sup>-1</sup> (not shown).

## Acknowledgments

We thank B. Mathiasch for recording the infrared spectra, K. Eberhardt and P. Thörle for the determination of the iron content by neutron activation analysis. We cordially thank M. Colussi for the DSC and TGA measurements and Dr. Christian Baerlocher for the XRD measurements (both ETH Zürich). We are grateful for financial support from the Deutsche Forschungsgemeinschaft (DFG), Program No. 1137 (Molecular Magnetism) and the Fonds der Chemischen Industrie.

- [1] P. Gütllich, H. A. Goodwin in *Spin Crossover in Topics in Current Chemistry*, Springer-Verlag, Berlin, Heidelberg, New York, **2004**, vol. 233–235.  
 [2] P. Gütllich, A. Hauser, H. Spiering, *Angew. Chem. Int. Ed. Engl.* **1994**, *33*, 2024–2054.  
 [3] H. Spiering, N. Willenbacher, *J. Phys.: Condens. Matter* **1989**, *1*, 10089–10105.

- [4] N. Willenbacher, H. Spiering, *J. Phys.: Condens. Matter* **1988**, *21*, 1423–1439.  
 [5] Y. Galyametdinov, V. Ksenofontov, A. Prosvirin, I. Ovchinnikov, G. Ivanova, P. Gütllich, W. Haase, *Angew. Chem. Int. Ed.* **2001**, *40*, 4269–4271.  
 [6] A. B. Gaspar, V. Ksenofontov, M. Seredyuk, P. Gütllich, *Coord. Chem. Rev.* **2005**, *249*, 2661–2676.  
 [7] M. Seredyuk, A. B. Gaspar, V. Ksenofontov, S. Reiman, Y. Galyametdinov, W. Haase, E. Rentschler, P. Gütllich, *Chem. Mater.* **2006**, *18*, 2513–2519.  
 [8] J. F. Létard, P. Guionneau, L. Goux-Capes in *Topics in Current Chemistry* (Eds.: P. Gütllich, H. A. Goodwin), Springer-Verlag, Berlin, Heidelberg, New York, **2004**, vol. 235, 221–249.  
 [9] J. A. Real, A. B. Gaspar, V. Niel, M. C. Munoz, *Coord. Chem. Rev.* **2003**, *236*, 121–141.  
 [10] A. Galet, A. B. Gaspar, M. C. Munoz, G. V. Bukin, G. Levchenko, J. A. Real, *Adv. Mater.* **2005**, *17*, 2949–2953.  
 [11] J. A. Real, A. B. Gaspar, M. C. Munoz, *Dalton Trans.* **2005**, 2062–2079.  
 [12] A. Hauser, J. Adler, P. Gütllich, *Chem. Phys. Lett.* **1988**, *152*, 468–472.  
 [13] Y. Maeda, M. Miyamoto, Y. Takashima, H. Oshio, *Inorg. Chim. Acta* **1993**, *204*, 231–237.  
 [14] A. D. Schlüter, J. P. Rabe, *Angew. Chem. Int. Ed.* **2000**, *39*, 864–883.  
 [15] H. Frauenrath, *Prog. Polym. Sci.* **2005**, *30*, 325–384.  
 [16] T. Fujigaya, D.-L. Jiang, T. Aida, *J. Am. Chem. Soc.* **2005**, *127*, 5484–5489.  
 [17] M. Balasubramanian, J. G. Keay, E. F. V. Scriven, *Heterocycles* **1994**, *37*, 1951–1975.  
 [18] A. Horváth, *Synthesis* **1995**, *9*, 1183–1189.  
 [19] C. Hawker, J. Fréchet, *J. Am. Chem. Soc.* **1990**, *112*, 7638–7647.  
 [20] Z. Yu, C. Li, X. Z. You, H. Spiering, P. Gütllich, Y. F. Hsia, *Mater. Chem. Phys.* **1997**, *48*, 150–155.  
 [21] J. Jung, H. Spiering, Z. Yu, P. Gütllich, *Hyperfine Interact.* **1995**, *95*, 107–128.  
 [22] C. M. Grunert, K. Eberhardt, P. Gütllich, P. Thörle, *Annual Report*, **2005**, Institut für Kernchemie, Johannes Gutenberg University, Mainz, **2006**.  
 [23] G. Socrates in *Infrared and Raman Characteristic Group Frequencies*, third ed., John Wiley & Sons, Chichester, **2001**.

Received: August 5, 2007

Published Online: February 11, 2008